On the use of vibration signal analysis for industrial quality control

Marco Cavallari, Gianluca D'Elia, Simone Delvecchio, Marco Malagò,
Emiliano Mucchi, Giorgio Dalpiaz
Engineering Department in Ferrara (EnDIF), University of Ferrara, Italy
E-mail: giorgio.dalpiaz@unife.it

Keywords: Vibration, condition monitoring, quality control, polyurethane wheels, helical gears, diesel engines, cold test.

SUMMARY. Vibration signals can be successfully captured and analysed for quality control at the end of the production line. Various signal processing techniques and their applications are presented in this paper. These applications demonstrate the importance of selecting proper signal processing tools in order to extract the most reliable information from the signals.

1 INTRODUCTION

In industrial manufacturing rigorous testing is used to ensure that the delivered products meet their specifications. In the last few years, a great effort has been put into automating fault detection by using vibration measurements and processing techniques, due to its non-intrusive character and ability to detect a wide range of mechanical faults. In industrial environments there is an increasing demand for automatic on-line systems which are able to classify final products as pass or fail and/or to diagnose faults. Firstly, the monitoring procedure involves the acquisition of vibration signals by means of piezo-electric accelerometers. Since the selection of the acquisition parameters is critical, this data acquisition step is not of minor importance. Sometimes, several operations (i.e. correct selection of time histories, averaging and digital filtering) are needed in order to separate the most informative part of the signal from the environmental noise (electrical and mechanical). Secondly, signal processing techniques have to be implemented by taking into account the characteristics of the signal and the type of machine from which the signal is being measured (i.e. rotating or alternative machine with simple or complex mechanisms). Finally, several features have to be extracted in order to assess the physical state of the machine or to detect some incipient defects and to determine the causes of their presence.

Mechanical faults in machines often show their presence through abnormal vibration signals, thus techniques for machine condition monitoring based on the analysis of these signals are widely used [1]-[2]. However, most studies have been carried out on simple mechanical parts, such as gears and rolling bearings, having well-determined dynamic characteristics. Therefore, gearbox condition monitoring and bearing defect analysis using vibration signatures are extensively reported ([3]-[4] among a wide range of References). Moreover, some works related to the condition monitoring of machining processes are present in literature ([5]-[6] refer to the drilling process as an example).

The aim of this paper is to present some quality control applications that are primarily based on vibration analysis. The use of processing techniques that can be considered well suited for implementation in on-line monitoring equipment at the end of the production line is proposed. The presented applications are: (a) the detection of contamination faults in polyurethane wheels; (b) tooth fault detection in helical gears; (c) the detection of assembly faults in diesel engines by means of cold test technology.

2 DETECTION OF CONTAMINATION FAULTS IN POLYURETHANE WHEELS

The first application deals with heavy-duty wheels that are mainly mounted in automatic vehicles; they are composed of a polyurethane tread and a cast iron hub. A thin coating of adhesive pastes the tread on the hub while two roller bearings couple the hub with the shaft. The application of the adhesive between the polyurethane tread and the cast iron hub represents the most critical assembly phase of these heavy-duty wheels, due to the fact that is completely realized by an operator. Therefore it is easy to understand that the contamination of the link area between polyurethane and cast iron is quite frequent. Four types of faulty wheels have been manufactured "ad hoc" with anomalies that mimic the real ones. Such anomalies consist in zones of different dimensions where incorrect adherence between tread and hub takes place.

Figure 1 depicts the artificial faults: defect A1 and A2 present an extension of 1 and 2 cm in tangential direction respectively, for the whole tread width, whilst A3 and A4 are localized in the centre of the interface tread/hub with an extension of 1 cm and 2 cm in tangential direction, respectively. For each defect type, three wheels have been tested in order to obtain more reliable results. Moreover seven healthy wheels (HW) have been also tested in order to identify a reference pattern that represents the normal condition.

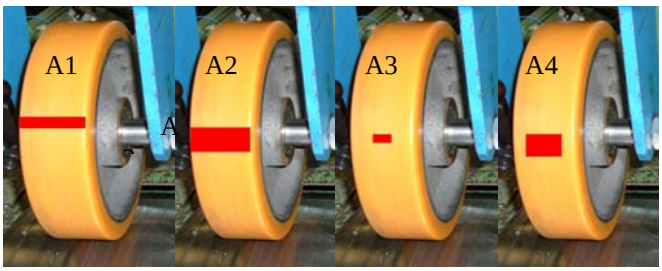

Figure 1: Defect of different dimensions, defined as A1, A2, A3 and A4.

2.1 *Experimental results and discussion*

The test bench used to perform the measurements is made up of a bottom support, including a drum driven by an electrical motor controlled by inverter, and an upper part composed of two hydraulic pistons that apply load to the wheel under test, as shown in Figure 2(a). Tests are carried out at two different drum speeds (low and high) and three different loads (low, medium and high). After a few preliminary analyses with different transducers (i.e. accelerometer, load cells, AE sensor, microphone), tri-axial accelerometer PCB 356A01 (frequency range 1-10000 Hz) has been identified as the best sensor in terms of simplicity in mounting and fast response to impulsive events. The vibration signals have been acquired with sample frequency of 20480 Hz for a duration of 64 s, by means of a LMS SCADAS 310 front-end, controlled by the software LMS Test.Lab. Simultaneously with the acquisition at constant sample frequency, an off-line computed order tracking analysis has been also performed in order to calculate the Time Synchronous Average (TSA) of the measured signal (Figure 3).

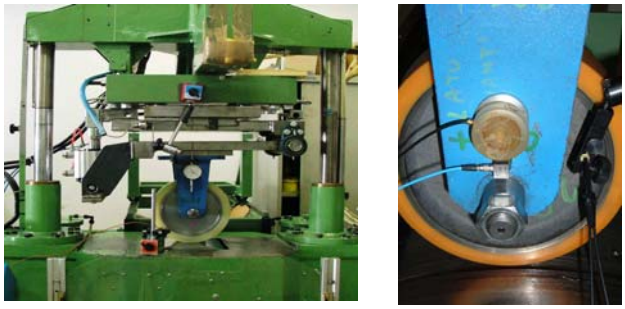

(a) (b)

Figure 2: (a) Test bench; (b) tested wheel and transducers.

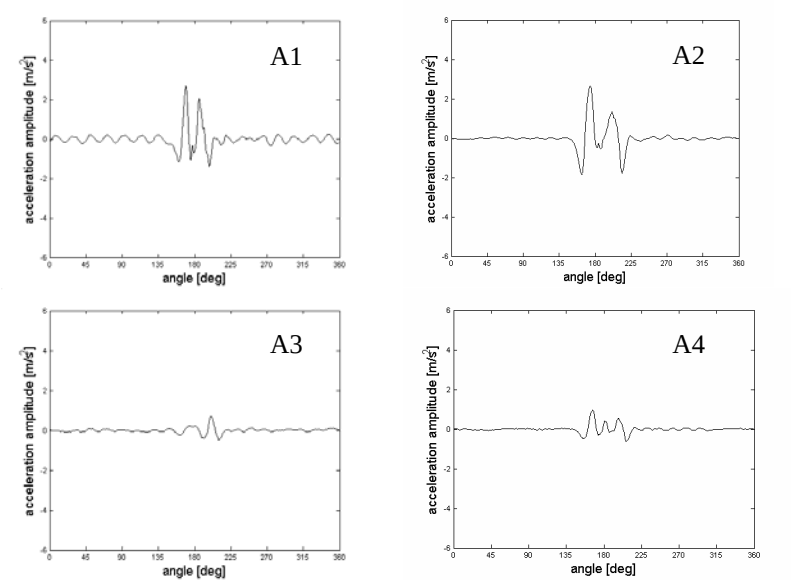

Figure 3: TSA of the acceleration signal for defects A1, A2, A3 and A4 at the test condition of low speed and high load.

This technique [7] requires the measurement of a one-per-revolution tachometer signal, i.e. a signal phase-locked with the angular position of one rotating element in the system. Two optical tachometer sensors (KEYENCE-LVS series) have been used to synchronise the acquisitions with both wheel and driving drum revolutions.

Concerning fault detection, the Kurtosis coefficient [8] extracted from the TSA vibration signal is well suited in highlighting localized faults, due to the fact that it assumes high values in signals that present few localized peaks, as occurs for wheels with anomaly, see Figure 3. Therefore, this technique can be a powerful and simply tool in vibration-based monitoring. Table 1 puts in evidence the Kurtosis coefficient values for all the defect types, evaluated at low speeds and high loads. As one can clearly see, the Kurtosis coefficient presents high values for the faulty wheels, while for healthy wheels it presents small values, less than 4. Table 2 shows that the test

conditions have a strong influence on Kurtosis values. In fact, it can be noted that the Kurtosis coefficients at higher speeds and lower loads are smaller than the Kurtosis coefficients at lower speeds and higher loads listed in Table 1. Furthermore, at higher speed and lower loads (see Table 2), the faulty wheels can not be clearly identified by using the Kurtosis coefficient only (defect A3 exhibits Kurtosis coefficient smaller than healthy wheels).

Table 1: Kurtosis of the TSA at the test condition of low speed and high load for defect types A1, A2, A3 and A4 and for healthy wheels (HW).

	A1	A2	A3	A4	HW
Kurtosis of the TSA	**16.01**	**13.17**	**12.01**	**13.26**	**3.27**

Table 2: Kurtosis of the TSA at the test condition of high speed and low load for defect types A1, A2, A3 and A4 and for healthy wheels (HW).

	A1	A2	A3	A4	HW
Kurtosis of the TSA	**6.03**	**7.12**	**3.25**	**4.12**	**3.27**

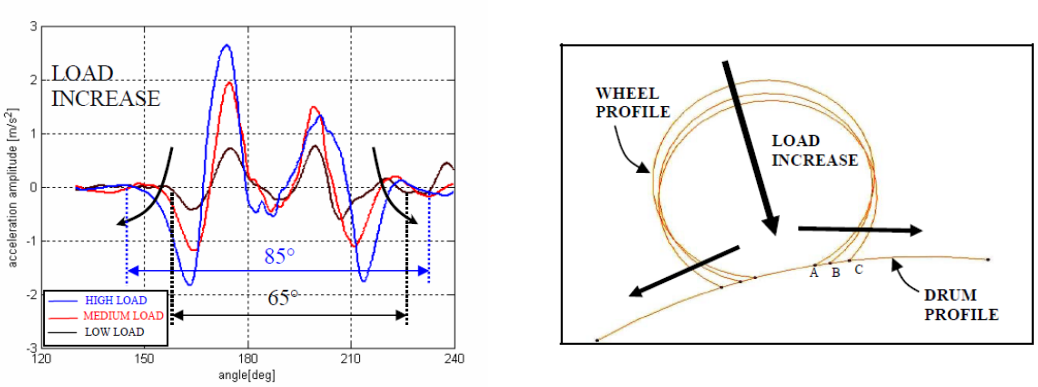

(a) (b)

Figure 4: (a) TSA of the acceleration signal for defect A2 at different loads (low, medium, high) at low speed in the angle range 120°- 240°; (b) sketch of the variation of contact area with the load increase.

Observing the zoom of typical TSA signals depicted in Figure 4(a), it can be easily noted that they are mainly composed of two impulsive events in each wheel rotation. These acceleration peaks are probably due to a double impact that happens when the fault area comes into contact and then exits the contact between the wheel and the drum. Moreover, it can be observed that different loads give different angular extensions of the transient event. In fact, a load variation produces a variation in the contact area size that affects the transient event duration. Figure 4(b) tries to explain how the contact area at different loads changes: in particular, point A represents the extreme of the contact area at low load conditions, involving a smaller surface and angular extension of the contact. On the other hand, point C represents this extreme in the highest load condition, determining the largest contact area and therefore involving the largest wheel angular extension. Figure 4(a) shows the TSA vibration signals obtained for defect A2 at three different loads (low, medium, high) and the same speed. It is clearly confirmed that the angular extension of the transient event becomes wider as load increases. As a matter of fact, the impulsive phenomena

(start/end contact of the non-pasted surfaces) related to the high load condition correspond to wheel rotation of approximately 85°, while at the low load condition only to 65°. Furthermore, the first contact point between the wheel and the drum is anticipated as the load increases while the last contact point is postponed. Moreover, Figure 4(a) shows that the peak amplitude becomes higher as the load increases, while the peak distance is not significantly influenced by the load and essentially depends on the defect type (see Figure 3).

On the basis of the presented results it can be concluded that the production of heavy duty wheels could be efficiently monitored through vibration signal analysis. A significant contribution to polyurethane wheel quality control can be achieved by TSA signal analysis and the calculation of simple statistical metrics. It also has to be highlighted that test conditions significantly influence the amplitude of the signal peaks and the angular extension of the transient event. On the other hand, the defect size influences the distance between peaks. More details can be found in [9].

3 TOOTH FAULT DETECTION IN HELICAL GEARS

The second application assesses the use of TSA vibration signal for the on-line vibration quality control of gear unites. The diagnostic capabilities of this simple technique have been tested on the basis of experimental results concerning two different tooth faults in helical gears: poor tooth surface quality and presence of tooth face bumps. The first fault condition concerns the presence of oxide residuals on the tooth surface due to the heat-treatment and the grinding process. The second one is caused by gear tooth impacts during gear conveyance before the heat treatment, see Figure 5(b). During the test campaign the faulty gears have been mounted on the first stage of a gear unit and the vibration signals have been acquired from the gearbox case.

3.1 *Experimental results and discussion*

Concerning fault detection, two statistical parameters, i.e. root-mean-square (RMS) and Kurtosis, extracted from faulty and sound TSA vibration signals have been evaluated in order to asses a reliable quality control strategy. The experimental apparatus (see Figure 5(a)) consists of a base, including two induction motors controlled by inverters and a gear unit. The driving induction motor is controlled in feedback speed loop, whilst the loading motor is controlled in feedback torque loop. The gear unit contains two spur gear pairs, one having 18 and 71 teeth, the other one 12 and 55 teeth, giving a global speed reduction ratio of 18.1. More details concerning the test bench design can be found in [10].

Three kinds of test are performed:

- Test 1: all gears in sound condition;
- Test 2: the first stage gearbox pinion (18 teeth) exhibiting several oxide residuals on tooth faces, so poor tooth surface quality (distributed fault);
- Test 3: the first stage gearbox wheel (71 teeth) showing tooth face bumps (localized fault).

The results presented in this work have been obtained with a nominal driving motor speed of 3000 rpm (50 Hz) and a output shaft nominal torque of 36.6 Nm. The vibration signal is captured from the gearbox case by means of a Brüel & Kjær piezoelectric accelerometer mounted close to the bearing support of the first stage pinion in the radial direction.

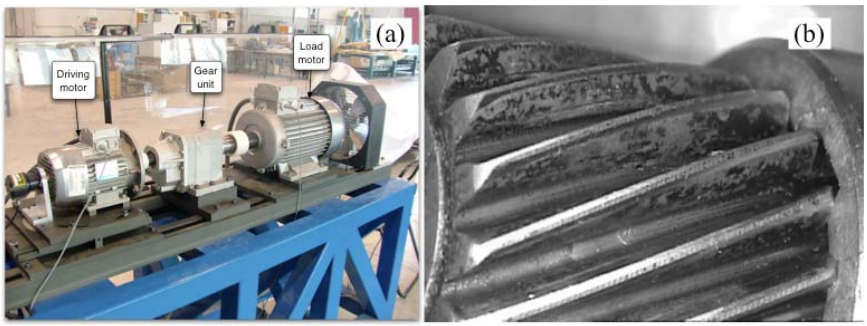

Figure 5: (a) Test bench for gear units and (b) example of a tested gear.

The sample frequency was 32800 Hz, whilst the acquisition time was 60 s. In all the tests the TSA vibration signal is calculated over 80 revolutions for both first stage pinion and wheel, obtaining both pinion TSA and wheel TSA. Figure 6(a) and Figure 6(b) plot the TSA of the first stage pinion and wheel for Test 1, which can be taken as a reference for the detection procedure. In particular, it is possible to notice that the main signal component is the meshing frequency and no signal alteration can be observed. Figure 6(c) shows the TSA of the first stage pinion for Test 2, concerning poor tooth surface quality. Comparing Figure 6(a) and Figure 6(c) it is possible to notice that this type of fault gives rise to an increase of the mean amplitude vibration level without any local alteration. Therefore by the visual inspection of the TSA this type of fault can not be surely identified and so further analyses have to be performed, i.e. evaluation of statistical parameters of the TSA signal. Concerning Test 3, the TSA of the first stage wheel is depicted in Figure 6(d). It is possible to notice a clear local alteration of the vibration signal at about 230 degrees due to the engagement of the faulted tooth with bumps.

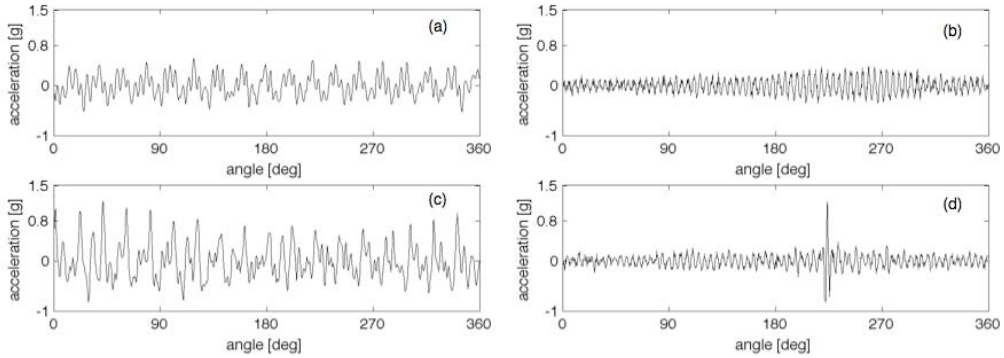

Figure 6: Time-synchronous averages for the three tests: (a) Test 1: pinion TSA in sound condition, (b) Test 1: wheel TSA in sound condition, (c) Test 2: pinion TSA with pinion distributed fault and (c) Test 3: wheel TSA with wheel localized fault.

Here it is clearly evident that the TSA seems a pivotal tool in revealing local alterations, i.e. localized fault in gear, nevertheless this techniques is not enough to reveal distributed faults. Moreover, in order to assess the presence of a defect a visual inspection of the TSA is needed; thus such a technique is not suitable to be implemented in an automatic monitoring system at the end of

the production line. Ergo, for quality control purposes, we can link this achievement to the analysis of statistical parameters of the TSA signal, i.e. RMS and Kurtosis. As a matter of fact these parameters are of simple interpretation and they are linked to different physical properties of the analyzed signal. In particular, RMS takes into account the energy conveyed by signals and so it can be considered as a useful tool in order to detect an increase of the mean signal amplitude (distributed faults). On the other hand Kurtosis is exceedingly sensitive to local signal alteration (localized faults). Table 3 summarises the RMS and the Kurtosis values for both pinion and wheel TSA of the three different tests.

Table 3: RMS and Kurtosis values of the TSA for the three tests.

	Pinion TSA		Wheel TSA	
	RMS [g]	Kurtosis	RMS [g]	Kurtosis
Test 1 (pinion and wheel in sound condition)	**0.21**	**2.39**	**0.14**	**2.52**
Test 2 (pinion distributed fault)	**0.35**	3.15	0.19	2.60
Test 3 (wheel localized fault)	0.13	2.80	0.13	**17.34**

It is well know that these statistical parameters evaluated on the TSA signal, have to be compared on the basis of the same mechanical component, i.e. pinion or wheel. As a matter of fact TSA in practice extracts from the signal the genuine portion containing only the components which are synchronous with the revolution of the specific gear in question. Therefore, the statistical parameters evaluated on the pinion TSA signal and on the wheel TSA signal, differ because they are evaluated on the basis of different signal components.

As reported in Table 3, there is an increase of the RMS value of the pinion TSA for Test 2 with respect to Test 1 (i.e. 0.35 g vs. 0.21 g), whilst the RMS of the wheel TSA does not show remarkable changes. Such an increase highlights the poor surface quality of the tooth pinion. Concerning Test 3 (wheel localized fault) the RMS of both pinion and wheel TSA's does not reveal the fault presence, in fact the energy conveyed by signal remains roughly the same (see Figure 6(b) and Figure 6(d) for the wheel TSA). On the other hand, the Kurtosis of the wheel TSA for Test 3 shows a marked increase with respect to Test 1 (i.e. 17.34 vs. 2.52), highlighting the presence of a localized fault on the first stage wheel.

Concerning this second application, we can consider TSA as a pivotal starting point for on-line gear quality control. However this techniques has to be linked to proper statistical parameters, such as RMS value or Kurtosis coefficient, in order to detect poor tooth surface quality or localized gear tooth faults. In particular, because RMS value accounts for the energy conveyed by the signal, it is well suited for distributed fault localization, while Kurtosis coefficient, which is sensitive to local signal alterations, is a pivotal tool for the monitoring of localized faults.

4 DETECTION OF ASSEMBLY FAULTS IN DIESEL ENGINE COLD TESTS

The latter application addresses the use of basic signal processing tools as means for the quality control of assembly faults in diesel engines through the cold test technology.

Nowadays, the main part of engine manufacturers tests their engines by means of "hot tests", i.e. tests in which engine is firing. Hot tests mainly aim to determine engine performances. Recently some companies have introduced "cold tests" aiming at identify assembly anomalies by means of torque, pressure and vibration measurements: this method has to be further improved.

In hot tests, anomalies are detected through the deterioration of the engine performances. Moreover vibration analysis is sometimes used to detect faults affecting combustion efficiency.

Cold tests are more oriented to identify the sources of anomalies since they are not affected by noise and vibration due to the firing.

The fault detection and diagnosis of i.c. engines can be carried out using different strategies. One strategy can consist in modelling the whole mechanical system using lumped or finite element methods in order to simulate several faults and compare the results with what the experimental tests found. Another strategy can adopt signal processing techniques in order to obtain features or maps that can be used to detect the presence of the defect. Regarding this, a decision algorithm is needed for a visual or automatic detection procedure. Moreover the maps can be also analysed for diagnostic purposes. This method is the most commonly used and well suited for the judgment of expert technicians. In this paper we try to investigate the problem of obtaining a strategy for the pass/fail decision at the end of the assembly line.

4.1 *Experimental results and discussion*

As presented in Refs. [10]-[13], the normalized time histories of acceleration signals concerning diesel engines can be represented as symmetrized dot polar (SDP) graphs. The formulation used for the transformation of a discrete signal to a polar coordinate graphs and the properties of this method are described in detail in [14]. Examples of the results are shown in Figure 7 and Figure 8. In order to implement this technique in the cold test procedure for fault detection, it is necessary to develop an image correlation system. The authors applied the algorithm of edge detection, illustrated in [14], which represents the most common approach for detecting meaningful discontinuities in intensity values.

The basic idea behind edge detection is to find the points where the intensity rapidly changes. For each case, by applying this edge detection algorithm on the image of the visual symmetrized dot polar graph, the result will be a boolean matrix with entries equal to 1 (represented as white pixels in the grey scale) located at the edge points, detected on the image, and entries equal to 0, (black pixels) located elsewhere (Figure 7(c)).

The goal is to identify a reference pattern that represents the normal condition and then compare the images obtained from all the test engines with this ‘healthy pattern’ by means of a similarity parameter. Among many possibilities, this parameter was chosen as the percentage of common white pixels with respect to the total number of white pixels in the healthy engine pattern. Hereafter, this parameter will be called correlation.

In order to set the detection threshold for the correlation, firstly the correlation parameter is calculated for all the couples of engines from a sample of 21 healthy engines: the engine that presents the minimum correlation with each other is assumed as the reference pattern, unique for all investigations, and the corresponding minimum correlation of 25.08% is fixed as the correlation threshold (CT). This pattern is compared with the images obtained from different faulty engines and so the correlations are calculated, verifying if they are lower than the CT in order to discriminate the faulty condition from the normal one.

Hereafter only the result concerning a specific fault is shown, as example. It deals with a connecting rod with incorrectly tightened screws: the rod screws are only tightened with the preload of 3 kgm, instead of the correct torque of 9 kgm.

Table 4 shows that this faulty engine gives a percentage of common white pixels lower than the CT. Similar results were found for other faulty conditions. It can be concluded that the percentage of common white pixels between each pattern and the reference one can be considered as a reliable parameter. Thus, it seems that this technique exhibits high sensitivity to faults, presenting some advantages, as fast computational implementation and easy output evaluation.

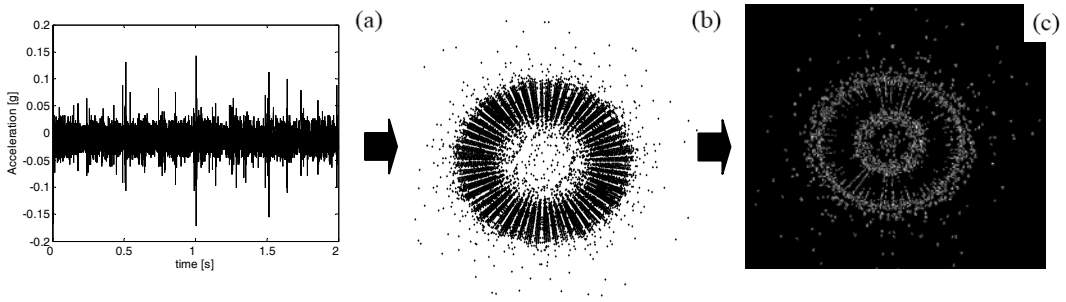

Figure 7: SDP method: (a) time input waveform; (b) symmetrized dot polar graph and (c) image obtained after the application of edge detection algorithm.

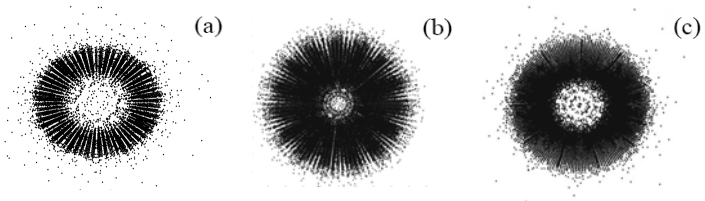

Figure 8: Symmetrized dot polar graphs: (a) healthy engine (reference pattern); (b) and (c) faulty engines.

Table 4: Symmetrized dot polar patterns: correlation values.

Comparison between symmetrized dot polar patterns	**Percentage of common white pixels [%]**
Healthy engine - Healthy engine	25.08 (CT)
Healthy engine - Faulty engine (incorrectly tightened rod screws)	10.80

5 CONCLUDING REMARKS

This paper describes some applications of vibration analyses for the quality control of mechanical devices at the end of the production line. The following conclusions can be achieved based on the presented results.

- Vibration signal is useful for quality control of the above-described applications, but it should be properly processed in order to obtain reliable information.
- In case of rotating machines, Time Synchronous Average can be considered as a powerful tool in detecting the presence of faults. It also permits the characterization of the source of alteration.
- The quality control at the end of assembly line requires the assessment of simple parameters that can be easily used for implementing a strategy of pass/fail decisions.
- Since the test conditions affect the robustness of the results it is recommended to select them in order to make the output vibration signal rich in informative characteristics.

ACKNOWLEDGEMENTS

This work has been developed within the laboratory of research and technology transfer InterMech (Division Acoustics and Vibrations - LAV) realized through the contribution of Regione Emilia Romagna - PRRIITT misura 3.4 azione A.

References

[1] Braun, S. J., *Mechanical Signature Analysis*. Academic Press, London (1986).

[2] Collacot, R.A., *Vibration Monitoring and Diagnostic*. Wiley, New York (1979).

[3] McFadden, P.D.,"Examination of a technique for the early detection of failure in gears by signal processing of the time domain average of the meshing vibration". *Mechanical Systems and Signal Processing*, **1**(2), April, pp. 173–183 (1986).

[4] Randall, R.B., "A new method of modeling gear faults". *Journal of Mechanical Design*, 104, pp. 259–267 (1982).

[5] El-Wardanay, T.I., Gao, D., Elbestawi M. A., Tool condition monitoring in drilling using vibration signature analysis. *International Journal of Machine Tools and Manufacture*, 36(6), 687-711 (1996).

[6] Jantunen, E., A summary of methods applied to tool condition monitoring in drilling, *International Journal of Machine Tools and Manufacture*, 42, 997-1010 (2002).

[7] Dalpiaz, G., Rivola, A., Rubini, R., "Effectiveness and sensitivity of vibration techniques for local detection in gears", *Mechanical System and Signal Processing*, Vol.**14(3)**, 387-412 (2000).

[8] Delvecchio, S.,Dalpiaz, Niculita, O., Rivola, A., "Condition monitoring in diesel engines for cold test applications. Part I: vibration analysis for pass/fail decision", in *Ana C V Veira et oth. editors, Proceedings of the 20th International Congress & Exhibition on Condition Monitoring and Diagnostic Engineering Management*, Faro, Portugal, June 13-15, 2007 pp.197-206 (2007).

[9] Malagò, M., Mucchi, E., Dalpiaz, G., "Condition monitoring and diagnosis in heavy-duty wheels: a first experimental approach" in *Proceedings of the ASME 2009 International Design Engineering Technical Conferences & Computers and Information in Engineering Conference IDETC/CIE 2009*, August 30-September 2, 2009, San Diego, California, USA.

[10] G. Dalpiaz, G. D'Elia, S. Delvecchio, Design of a test bench for the vibro-acoustical analysis and diagnostics of rotating machines, in *Proceedings of the Second World Congress on Engineering Asset Management and the Fourth International Conference on Condition Monitoring 2007*, Harrogate, UK, 11-14 June 2007.

[11] Wu, J. D., and Chuang, C.Q., "Fault diagnosis of internal combustion engines using visual dot patterns of acoustic and vibration signals". *NDT&E International*, **38**, pp. 605-614 (2005).

[12] Shibata, K., Takahashi, A., and Shirai, T., "Fault diagnosis of rotating machinery through visualisation of sound signal". *Mechanical Systems and Signal Processing*, **14**(2), pp. 229-241 (2000).

[13] Delvecchio, S., D'Elia, G., Di Gregorio, R., Dalpiaz, G., On the monitoring and diagnosis of assembly faults in diesel engines: a case study, in *Proceedings of the ASME 2009 International Design Engineering Technical Conferences & Computers and Information in Engineering Conference IDETC/CIE 2009*, August 30-September 2, 2009, San Diego, California, USA.

[14] Gonzalez, R., Woods, R., and Eddins, S., *Digital Image Processing Using Matlab*. Prentice Hall (2004).